

**PICTORIAL ESSAY**

**Imaging Features of Alveolar Soft Part Sarcoma**

S Nicolaou,<sup>1</sup> J Hagel,<sup>1</sup> PL Munk,<sup>1</sup> WC Torreggiani,<sup>1</sup> JJ Dubec,<sup>1</sup> MJ Lee,<sup>1</sup> JX O’Connell<sup>2</sup>

<sup>1</sup>Department of Radiology, <sup>2</sup>Department of Pathology, Vancouver General Hospital, Vancouver, Canada

**ABSTRACT**

*Alveolar soft part sarcoma is a rare, highly vascular, soft tissue sarcoma. It usually presents as a slow growing, painless lesion in the lower extremities of young adults. Bone invasion is rare. In this pictorial essay, we present the imaging features, approach to differential diagnosis, and prognosis of alveolar soft part sarcoma, with and without bone invasion.*

**Key Words:** Alveolar soft part sarcoma, Angiography, Computed tomography, Differential diagnosis, MRI, Prognosis

**INTRODUCTION**

Alveolar soft part sarcoma (ASPS) is a highly vascular malignancy that constitutes less than 1% of soft tissue sarcomas.<sup>1,2</sup> This tumour typically occurs in the second to fourth decades of life, and has a slight female predominance.<sup>2</sup> Clinically, ASPS most commonly presents as a deep, painless, slow growing, soft tissue lesion. Due to the vascularity of the tumour, the mass may be pulsatile or associated with an audible bruit, and is often mistaken for an arteriovenous malformation (AVM). The lesion most commonly occurs in the lower extremities. Other locations described include the upper extremities, head and neck, retroperitoneum, chest wall, and pelvis.<sup>3</sup> Despite the typically slow growth of ASPS, the high prevalence of metastases makes early clinical recognition of this tumour particularly important.<sup>4</sup>

Bony invasion is an uncommon feature of ASPS and has been described in only a few reports in the radiological literature. None have adequately displayed images involving bony destruction using both CT and MRI.<sup>5-9</sup>

In the following discussion, characteristic histological and imaging features of ASPS and the findings

associated with bone invasion will be illustrated. The images used were obtained from 4 patients (Table 1). The tumours were excised and confirmed histologically in all 4 patients, with bony invasion present in 3 of the cases.

**Table 1.** Features of 4 patients with a histological diagnosis of alveolar soft part sarcoma.

	Case 1	Case 2	Case 3	Case 4
Age	26	24	49	27
Sex	Female	Male	Female	Female
Location of lesion	Left thigh	Left lower limb	Right forearm	Left gluteal
<b>CT Findings</b>				
- Calcification	Not done	Not assessed <sup>a</sup>	Not assessed	Not assessed
- Soft tissue mass	Not done	+	+	+
- Bone invasion	Not done	+	+	None
- Enhancement	Not done	+	+	+
<b>MRI Findings</b>				
- SI on T1-WIs	Not done	High <sup>b</sup>	High	High
- SI on T2-WIs	Very high <sup>c</sup>	Very high	Very high	Very high
- SI on GRE sequence	Very high	Very high	Very high	Very high
- Flow voids	+	+	+	+
- Bone invasion	+	+	+	None
- Enhancement	+	+	+	+
	(dramatic)	(dramatic)	(dramatic)	(dramatic)
<b>Angiography</b>				
- A-V shunting	+	+	Not done	Not done
- Enlarged feeding artery	+	+	Not done	Not done
- Early draining vein	+	+	Not done	Not done
- Capillary staining	+	+	Not done	Not done

Abbreviations and notes: SI = signal intensity; T1-, T2-WIs = T1-, T2-weighted images; GRE = gradient-recalled-echo; A-V = arterio-venous; <sup>a</sup>only contrast studies performed; <sup>b</sup>SI higher than surrounding muscle, but lower than fat; <sup>c</sup>SI higher than fat.

**Correspondence:** Dr. S Nicolaou, Department of Radiology, Vancouver General Hospital, 899 West 12th Ave, Vancouver, British Columbia, V5Z 1M9, Canada.

Tel: (604) 875 4111; Fax: (604) 875 4723;

E-mail: snicola@vanhosp.bc.ca

Submitted: 13 June 2001; Accepted: 3 December 2001.

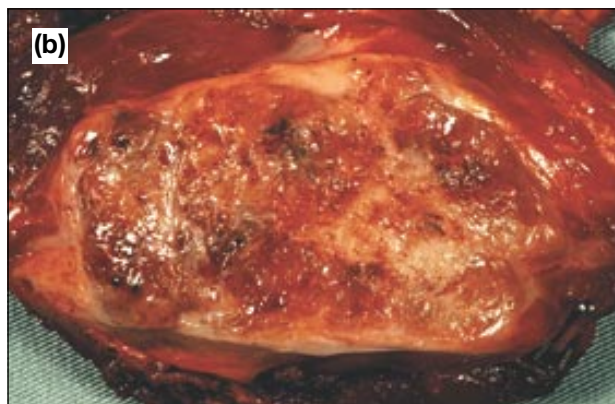
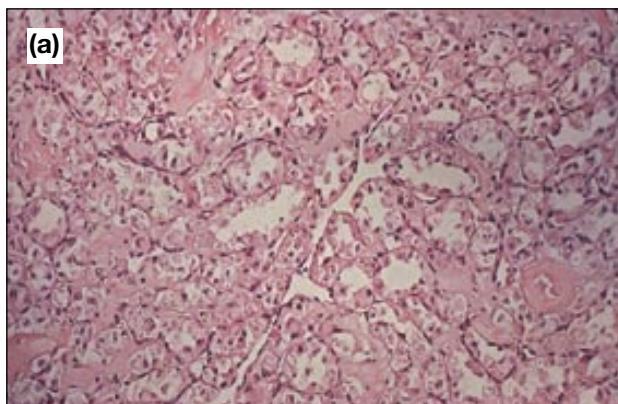


**Figure 1.** Typical appearance of alveolar soft part sarcoma. (a) On microscopy, the tumour shows nested growth. The tumour cells separate from each other producing the central 'empty spaces' that account for the descriptive designation of the tumour as 'alveolar'; (b) gross morphology. The tumour appears well-circumscribed and brown. The dark red regions represent the dilated vascular structures that are present throughout the tumour.

## DISCUSSION

### Pathology

ASPS was first comprehensively described by Christopherson et al in 1952.<sup>10</sup> The name refers not to its histological origin, but to the typical microscopic morphology of large granular cells organised in an alveoli-like array and separated by a rich vascular network (Figure 1a). Despite extensive investigation and considerable speculation, the histogenesis of ASPS continues to be a disputed issue half a century after its initial description.<sup>3</sup> Microscopically, the appearance may be mistaken for metastatic renal, adrenal, or hepatocellular carcinoma.<sup>11,12</sup> The gross specimen of this type of tumour is typically a well-circumscribed mass that is partly encapsulated (Figure 1b).<sup>4</sup>

### Plain Film

Prior to the widespread use of CT and MRI, evaluation of these tumours relied on plain film, nuclear medicine, and angiography. Occasionally, plain film radiography may show a soft tissue mass associated with punctate calcification, although this phenomenon was noted in only 2 of 11 cases reported by Lorigan et al.<sup>7</sup> When bone invasion occurs, ASPS produces an ill-defined, non-specific, lytic lesion on plain film (Figure 2).<sup>4</sup>



**Figure 2.** Film radiography (case 3). As with any other aggressive sarcomatous type lesion, alveolar soft part sarcoma demonstrates a non-specific pattern on plain film radiography. Here, the lateral view of the right forearm reveals a permeative and destructive bony lesion affecting the proximal and mid-diaphysis of the right radius.

### Angiography

Typical angiographic features include enlarged feeding arteries, early draining veins, capillary staining, arteriovenous shunting, and slow wash out (Figure 3).<sup>6,12</sup>



**Figure 3.** Angiography (case 1). This delayed image of a left femoral arteriogram reveals a highly vascular mass that is supplied by large, tortuous, feeding arteries arising from the left superficial femoral artery. The mass demonstrates prominent capillary staining with venous lakes and arteriovenous shunting, as well as prominent early draining veins. These findings are characteristic of a highly vascular soft tissue mass, such as alveolar soft part sarcoma.

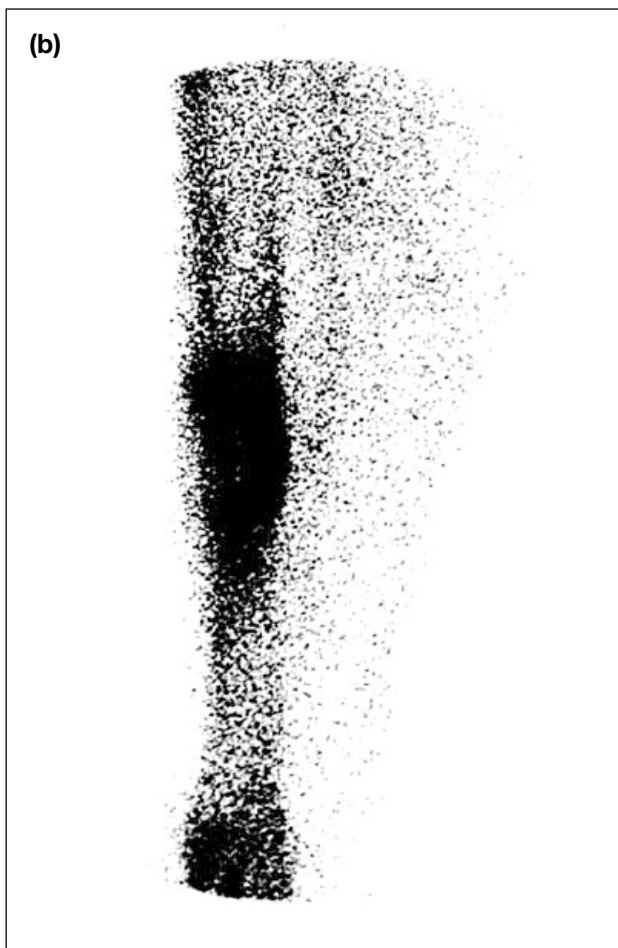
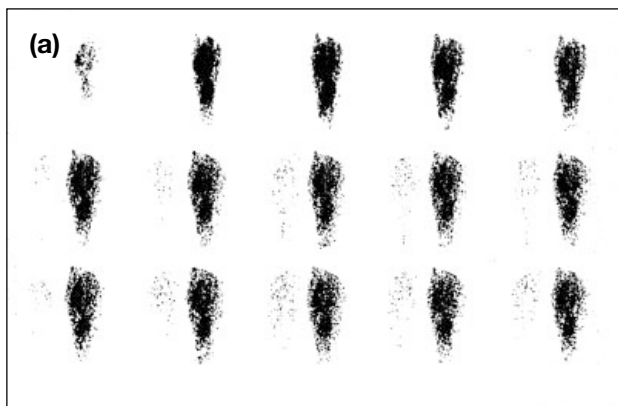


**Figure 4.** Nuclear medicine studies (case 1). (a) Dynamic phase images from a 99m-technetium bone scan demonstrate early increased radiopharmaceutical uptake, indicating the markedly vascular nature of this type of lesion; (b) delayed static images in the anterior projection reveal marked uptake of the isotope in the tibia that mimicks osteomyelitis.

**Nuclear Medicine**

On nuclear medicine studies, ASPS with bone invasion has non-specific findings, demonstrating increased radiopharmaceutical uptake on early and delayed images (Figure 4).<sup>9</sup> This feature can be seen in any other vascular mass or inflammatory process with bone involvement.



**Figure 5.** Enhanced axial CT scans of the gluteal region, taken using soft tissue window settings (120 kV, 260 mA, 5 mm thick, W=407, L=41), reveal a well-defined, highly enhancing soft tissue mass involving the medial aspect of the left gluteus maximus, and also demonstrate the extremely vascular nature of this type of sarcoma (case 4).

**Computed Tomography**

On unenhanced CT scans, ASPS generally displays an attenuation that is less than or equal to that of surrounding muscle. Tumour margins on CT images can vary from well-defined to infiltrating. Central necrosis can be seen in up to 75% of cases.<sup>4,11</sup> Due to the extremely vascular nature of this lesion, dramatic enhancement is seen with administration of iodinated contrast (Figure 5). Invasion of adjacent bone by ASPS is a rare feature. There have been a few reports in the radiological literature that have demonstrated bony invasion by these tumours using cross-sectional imaging.<sup>6,7</sup> CT clarifies the extent of bony invasion, presence of periosteal reaction, cortical erosion, and intramedullary extension (Figures 6 and 7).<sup>9</sup>

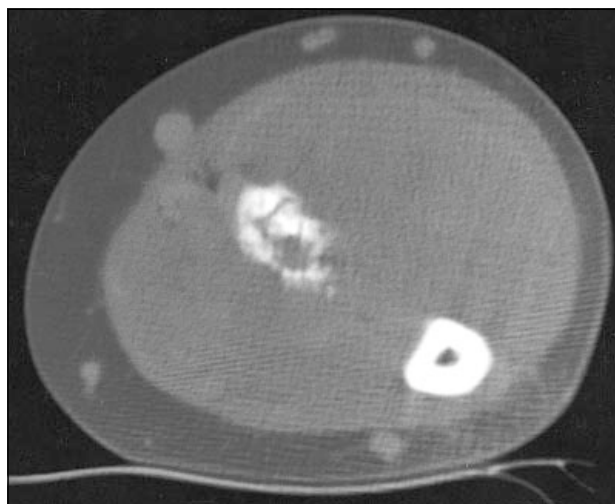


**Figure 6.** Enhanced axial CT scans of the same right forearm lesion as described in figure 2, taken using bone window settings (120 kV, 200 mA, 5 mm thick, W=450, L=50), clearly display evidence of bony destruction by the adjacent soft tissue mass, in keeping with bony invasion (case 3).



**Figure 7.** Enhanced axial CT scans of the gluteal region, taken using soft tissue window settings (120 kV, 200 mA, 5 mm thick, W=2000, L=250), reveal a heterogeneously enhancing soft tissue mass interposed along the proximal aspect of the left tibia and fibula. Note: these images show that resorption of the medial cortical margin of the proximal tibia has taken place (suggesting bony invasion), although this is better appreciated on subsequent MRI images (Figures 8-13). Areas of decreased attenuation presenting centrally within the mass correspond to foci of necrosis within the tumour (case 2).

### **Magnetic Resonance Imaging**

On unenhanced T1-weighted MRI images, the mass is usually of equal or higher signal intensity to that of adjacent muscle (Figure 8a). For example, Iwamoto et al reported 10 cases noting signal intensity greater than that of skeletal muscle on T1-weighted images.<sup>11</sup> Although the exact aetiology of the increased signal intensity is unclear, it is believed that this may be

attributed to slow flowing blood through the extensive vascular channels that are associated with this type of sarcoma. T2-weighted images demonstrate very high signal intensity — higher than that of fat and adjacent muscle (Figures 9, 10, and 11). Numerous serpentine flow voids are usually seen in T1- and T2-weighted images (better seen in T2-weighted images), representing enlarged feeding arteries and draining veins. Marked enhancement is seen with gadolinium administration, indicating the highly vascular nature of this lesion (Figures 8b and 8c).

Additional MRI sequences can be performed to further define the nature of this type of lesion. Short tau inversion recovery and gradient-weighted sequences, for example, reveal the mass to be of extremely high signal intensity. They also demonstrate the presence of numerous serpentine flow voids, which can be most

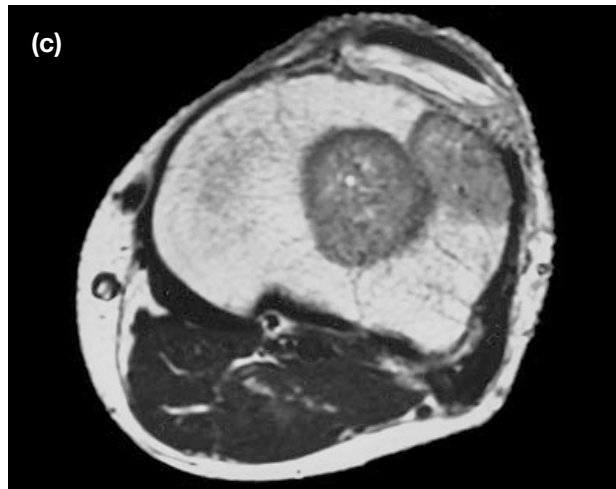
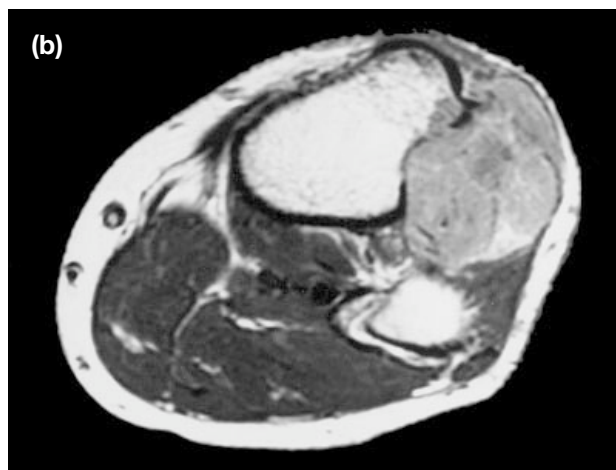
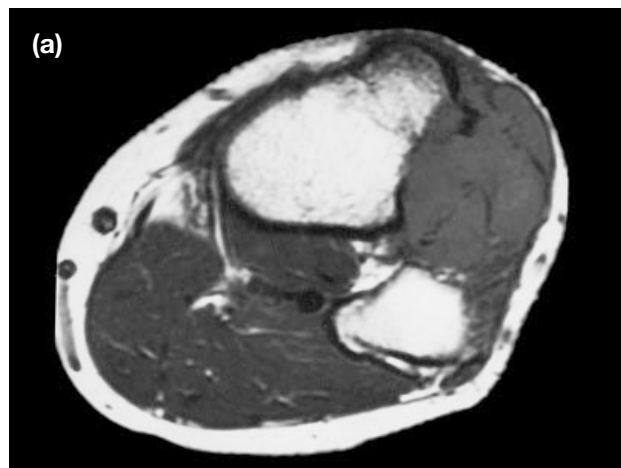


**Figure 8.** Non-enhanced (a) and gadolinium-enhanced (b and c) spin echo T1-weighted sequences of the left knee (TR 450, TE 16, FOV 17, 5 mm thick/1.0 space). The non-enhanced image reveals a 4 × 5 cm soft tissue mass interposed along the proximal aspects of the left tibia and fibula, which is of slightly higher signal intensity than that of adjacent muscle. On the gadolinium-enhanced images, heterogeneous enhancement of the lesion is identified. Resorption of the medial cortical margin of the proximal tibia is clearly depicted, along with the actual tumour invading the medullary cavity of the proximal tibial epiphysis and metaphysis. Both are consistent with bony invasion (case 2).

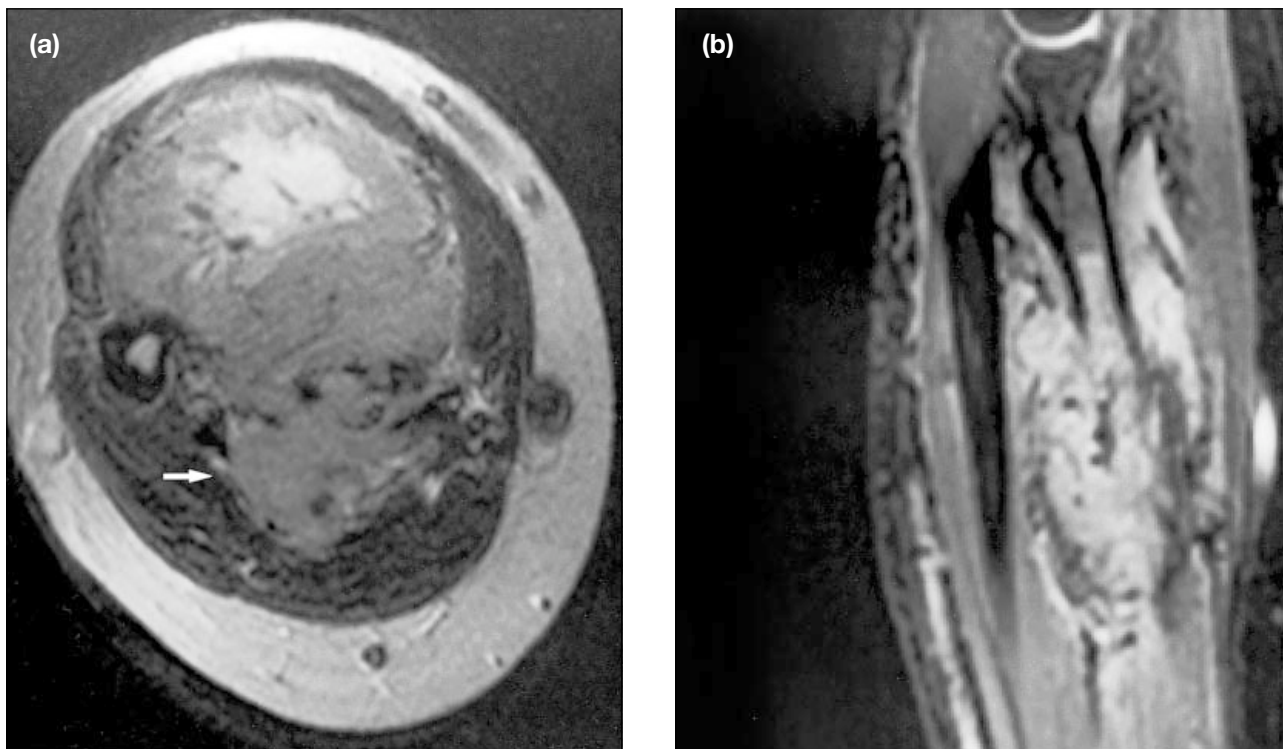


**Figure 9.** Transverse (a) and sagittal (b) fast spin echo T2-weighted sequences with fat saturation (TR 4000, TE 85, FOV 14, 5 mm thick/4.0 space, fat sat) of the proximal and mid-diaphyseal portion of the right forearm reveal a 6 × 4 cm soft tissue mass involving the flexor compartment. Breach of the interosseous membrane to involve the extensor compartment of the right forearm is also apparent [white arrow on (a)]. Its signal characteristics are higher than that of adjacent muscle. The lesion also demonstrates signal characteristics consistent with its being of a highly vascular nature. Centrally, the mass demonstrates this increased signal with numerous serpentine flow voids that represent vascular channels. On the sagittal view, increased signal within the radius is present, indicating bone invasion (case 3).

obvious at the margins of the lesion or may be found within the substance of the mass itself (Figures 12 and 13). On gradient-weighted sequences, haemosiderin deposition can also be seen, indicating previous haemorrhage.

The MRI scans of all our cases demonstrated breach of cortical bone by the adjacent soft tissue mass and high signal intensity within the intramedullary cavity. Each case was confirmed with pathology to discern between tumour invasion and bony oedema.

### Differential Diagnosis

It should be noted that differentiating ASPS from a slow flowing haemangioma can be difficult, as both lesions display high signal intensity on T1- and T2-weighted images. They can be distinguished from one another, however, by the presence in ASPS of flow voids — these are usually lacking in slow flowing haemangiomas. Enhanced CT can also help differentiate between these 2 lesions, as ASPS usually shows areas of hyperdensity at the periphery, with a central area of low attenuation indicating necrosis, whereas haemangiomas do not. ASPS has occasionally been misdiagnosed as a

high flow AVM. A previous report has suggested that the two can be definitively differentiated by angiography: whereas ASPS demonstrates a slow wash out of contrast material, an AVM demonstrates a rapid wash out. On CT, the findings of a significant soft tissue component, central necrosis, and bony invasion are all features that, if present, point towards ASPS, as opposed to an AVM. MRI can accurately differentiate ASPS from an AVM, as ASPS demonstrates high signal intensity on T1- and T2-weighted images, whereas an AVM shows low signal intensity.<sup>11</sup>

Vascular metastases, such as renal cell carcinoma, must also be considered in the differential diagnosis. Lastly, other types of primary soft tissue sarcomas that can invade bone or, conversely, primitive bone tumours that can invade soft tissues must be considered, although these are less likely to have the extreme vascularity that ASPS demonstrates.

### Prognosis and Management

Patient age, size of the tumour, and the presence of metastases are important prognostic factors in ASPS. In the series reported by Lieberman et al, the median



**Figure 10.** Coronal fast spin echo T2-weighted sequence with fat suppression (TR 3850, TE 105, FOV 20, 4 mm thick/0.0 space, fat sat) best depicts bony invasion by the high signal, lobular, soft tissue mass. There is clear depiction of high signal tumour involving the medullary cavity of the proximal tibial epiphysis, once more displaying evidence of bony invasion (case 2).

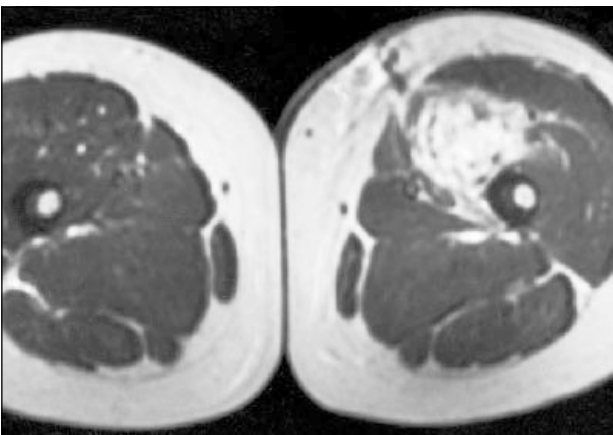


**Figure 11.** Axial spin echo T2-weighted sequences (TR 2000, TE 80, FOV 40, 10 mm thick/5.0 space) reveal a high signal, soft tissue mass present primarily within the vastus medialis. This mass displays numerous low signal tubular structures consistent with vascular flow voids, suggesting that it is highly vascular. There is irregularity of the medial cortical margin of the left femur at the level of the proximal diaphysis and metaphysis where the mass is seen to be in close apposition, suggesting bony invasion (case 1).

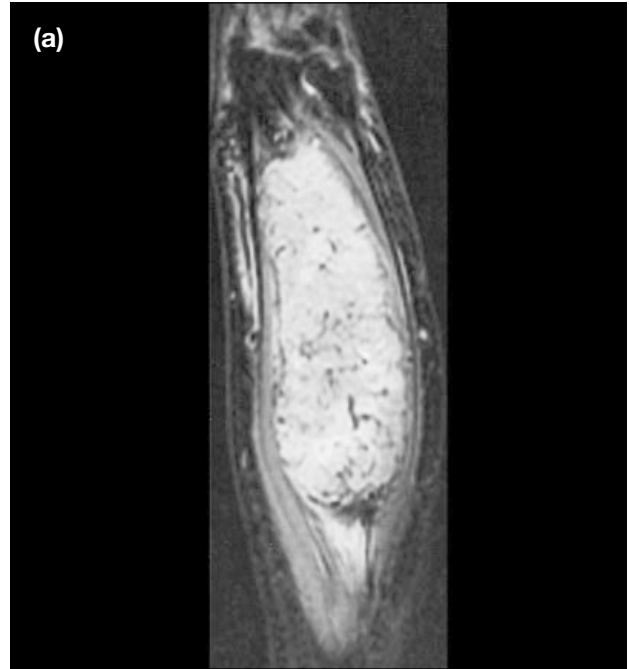


**Figure 12.** Sagittal inversion recovery [TR 2000, TE 16, TI 150, FOV 28, 5 mm thick/4.0 space] (a) and coronal gradient-weighted [TR 500, TE 15, FOV 28, 4.0 mm thick/0.0 space, flip angle 30°] (b) sequences of the right forearm reveal a highly attenuating soft tissue mass occupying both the flexor and extensor compartments. As was apparent in the fast spin echo T2-weighted sequence (Figure 9), this type of sequence again reveals the highly vascular nature of the soft tissue mass, demonstrating an increased signal and numerous serpentine, low signal foci consistent with vascular flow voids. Bony invasion, which is a rare finding associated with alveolar soft part sarcoma, is demonstrated within this example. There is increased signal present within the medullary cavity at the proximal and mid-diaphyseal level of the right radius, and this was confirmed on subsequent pathology to represent invasion of the bone (case 3).



**Figure 13 (a and b).** Coronal gradient-weighted sequence of the left femur (TR 600, TE 20, FOV 48, 5 mm thick/2.5 space, flip angle 20°) reveals a highly attenuating soft tissue mass adjacent to the proximal diaphyseal region. Consistent with bone invasion, which was confirmed on pathology, there is a high signal present within the medullary cavity of the left femur, which is continuous with the adjacent high-signal soft tissue mass (case 1).

survival rate of patients at 0 to 9 years of age was 20 years; at 10 to 19 years, it was 14 years; at 20 to 29 years, it was 6 years; and at age 30 or older, it was 5 years. Patients with a primary tumour that measured greater than 5 cm were also found to have shorter survival times than those with a mass measuring less than 5 cm.<sup>13</sup>

Metastases are common, being detected in about 20 to 25% of patients at the time of diagnosis. In particular, lung metastases are found in as many as 40% of cases at the time of diagnosis, with the brain and bone being other common sites of spread.<sup>13</sup>

Surgical excision with critical evaluation of the surgical margins is the primary therapeutic option for ASPS. In their review of half a century's worth of experience, Lieberman et al found no indication that chemotherapy or radiation therapy improved survival.<sup>13</sup> Hence, these therapeutic modalities might have a role for palliative purposes only.

## CONCLUSIONS

Although ASPS is a rare malignant neoplasm, it should be considered in the setting of a young patient presenting with a slow growing soft tissue mass of the lower extremities. Particularly on MRI, the lesion demonstrates increased signal intensity on T1- (non-enhanced) and T2-weighted images, numerous flow voids, and marked gadolinium enhancement; all of these features are consistent with a highly vascular tumour. Although bone invasion is a rare feature of ASPS, it can be concluded that this has occurred if CT and MRI images demonstrate a soft tissue mass that is associated with a periosteal reaction, bony oedema, and extensive cortical destruction.

## REFERENCES

1. Auerbach HE, Brooks JJ. Alveolar soft part sarcoma. A clinicopathologic and immunohistochemical study. *Cancer* 1987; 60:66-73.
2. Franz M, Enzinger SW. *Soft tissue tumors*. St.Louis: Mosby; 1995:1067-1093.
3. Ordonez NG. Alveolar soft part sarcoma: a review and update. *Adv Anat Pathol* 1999;6:125-139.
4. Temple HT, Scully SP, O'Keefe RJ, Rosenthal DI, Mankin HJ. Clinical presentation of alveolar soft-part sarcoma. *Clin Orthop* 1994;300:213-218.
5. Furey JG, Barrett DL, Seibert RH. Alveolar soft-part sarcoma: report of a case presenting as a sacral bone tumor. *J Bone Joint Surg Am* 1969;51:185-190.
6. Hermann G, Abdelwahab IF, Klein MJ, Kenan S, Lewis MM. Case report 796. Alveolar soft part sarcoma. *Skeletal Radiol* 1993;22:386-389.

7. Lorigan JG, O’Keeffe FN, Evans HL, Wallace S. The radiologic manifestations of alveolar soft-part sarcoma. *AJR Am J Roentgenol* 1989;153:335-339.
8. Evans HL. Alveolar soft-part sarcoma. A study of 13 typical examples and one with a histologically atypical component. *Cancer* 1985;55:912-917.
9. Munk PL, Connell DG, Muller NL, Lentle BC. Case report 501. Alveolar soft parts sarcoma with pulmonary metastases. *Skeletal Radiol* 1988;17:454-457.
10. Christopherson WM, Foote FW Jr, Stewart FW. Alveolar soft part sarcoma: structurally characteristic tumors of uncertain histogenesis. *Cancer* 1952;5:100-111.
11. Iwamoto YI, Morimoto N, Chuman H, Shinohara N, Sugioka Y. The role of MR imaging in the diagnosis of alveolar soft part sarcoma: a report of 10 cases. *Skeletal Radiol* 1995;24:267-270.
12. Radin DR, Ralls PW, Boswell WD, Lundell C, Halls JM. Alveolar soft part sarcoma: CT findings. *J Comput Assist Tomogr* 1984;8:344-345.
13. Lieberman PH, Brennan MF, Kimmel M, Erlandson RA, Garin-Chesa P, Flehinger BY. Alveolar soft part sarcoma: a clinico-pathologic study of half a century. *Cancer* 1989;63:1-13.

## Erratum

In the Review Article of the April-June 2001 issue of the *Journal of the Hong Kong College of Radiologists* (*J HK Coll Radiol* 2001;4(2):122-127), Figure 2 on page 124 was reprinted with permission from Reference 12 on page 127 — ‘Berlin NI, Wasserman LR. Polycythemia vera: a retrospective and reprise. *J Lab Clin Med* 1997;130:365-373.’ The legend of Figure 2 should read as:

**Figure 2.** Cumulative survival of patients in the three treatment arms of PVSG-01. Reprinted with permission.<sup>12</sup>

**and not**

**Figure 2.** Cumulative survival of patients in the three treatment arms of PVSG-01. Reprinted with permission.<sup>11</sup>

.....

In the How I Do It article (Recanalization of Superficial Femoral Artery Occlusion — The Subintimal Approach) of the July-September 2001 issue of the *Journal of the Hong Kong College of Radiologists* (*J HK Coll Radiol* 2001;4(3):226-230), the legend for the figure at the top left hand column on page 229 should read as:

**Figure 4.** The dilating catheter is advanced along the guidewire until the distal end reaches the true lumen. Re-entry into the true lumen is confirmed by injecting iodinated contrast.

**and not**

**Figure 5.** A postprocedure angiogram is performed through the arterial sheath with the extra-stiff guidewire in place. The typical spiral appearance of the subintimal neo-lumen can be seen.